

Micrometer-scale Domains in Fibroblast Plasma Membranes

Elishalom Yechiel and Michael Edidin

Biology Department, The Johns Hopkins University, Baltimore, Maryland 21218

Abstract. We have used the technique of fluorescence photobleaching recovery to measure the lateral diffusion coefficients and the mobile fractions of a fluorescent lipid probe, 1-acyl-2-(12-[(7-nitro-2-1,3-benzoxadiazol-4-yl)aminododecanoyl]) phosphatidylcholine (NBD-PC), and of labeled membrane proteins of human fibroblasts. Values for mobile fractions decrease monotonically with increasing size of the laser spot used for the measurements, over a range of 0.35–5.0 μm . Values for NBD-PC diffusion coefficients increase in part of this range to reach a plateau at larger laser spots. This variation is not an artifact of the measuring

system, since the effects are not seen if diffusion of the probe is measured in liposomes. We also find that the distribution of diffusion coefficients measured with small laser spots is heterogeneous indicating that these small spots can sample different regions of the membrane. These regions appear to differ in protein concentration. Our data strongly indicate that fibroblast surface membranes consist of protein-rich domains ~ 1 μm in diameter, embedded in a relatively protein-poor lipid continuum. These features appear in photographs of labeled cell surfaces illuminated by the expanded laser beam.

THE organization of membrane lipids and proteins, and the role of this organization in membrane function, are major topics in modern biology. The commonly quoted model of membrane structure posits a random distribution of membrane molecules (16), but does not rule out the possibility that membrane lipids and proteins may be organized into domains whose protein and lipid composition differ from the bulk of the membrane. Such domains, which measure on the scale of tens of micrometers, are found in the plasma membranes of many tissue cells, notably in functionally polarized cells (1, 4, 17). Evidence for smaller domains in less specialized surface membranes comes from experiments showing complex behavior of lipid labels in cell membranes different from the behavior of these probes in simple liposome membranes (9–11, 18–20). Such experiments often require determination of multiple values (e.g., of fluorescence lifetime) from single experimental curves, or depend upon the use of several different lipids or lipid analogs.

We now show that the lateral diffusion of a single species of lipid label, 1-acyl-2-(12-[(7-nitro-2-1, 3-benzoxadiazol-4yl)aminododecanoyl]phosphatidylcholine (NBD-PC),¹ gives strong evidence for the existence of lipid domains, in fibroblast plasma membranes. The diffusion coefficient and the mobile fraction of a single fluorescent lipid probe, NBD-PC, and of labeled membrane proteins, vary with the size of the laser spot used to probe the labeled surface. This variation

is not an artifact of the measuring system. Our data strongly indicate that fibroblast surface membranes consist of protein-rich domains ~ 1 μm in diameter, embedded in a relatively protein-poor lipid continuum.

Materials and Methods

Cells

Early-passage human skin fibroblasts (CCD; American Type Culture Collection, Rockville, MD) were grown in MEM (Gibco, Grand Island, NY), supplemented with 20% FCS (Reheis, Division of Armour Pharmaceutical Co., Tarrytown, NY). Cells were removed from dishes with chicken serum/trypsin/collagenase (2.5%:0.2%:0.002%). Fibroblasts at the sixth passage were plated onto glass coverslips for photobleaching measurements.

Labeling

Cell lipids were labeled with NBD-PC (Avanti Polar Lipids, Inc., Birmingham, AL) or with 1,1'-ditetradecyl-3,3',3'-tetramethylindocarbocyanine (diI C14) (Molecular Probes, Inc., Eugene, OR). Cell proteins were labeled with fluorescein-conjugated Fab fragments (Fl-Fab) (14) of a rabbit anti-human cell antibody which reacts well with mobile proteins of a variety of human cells (6).

Large Liposomes

Large liposomes were prepared by the method of Oku et al. (13).

Measurement of Lateral Diffusion

We used spot photobleaching (8) of labeled membranes to measure lateral mobility of labeled membrane components. In this experiment, an attenuated laser beam is focused on a labeled cell surface to define the area to be measured. Label is bleached by briefly removing the attenuation, therefore increasing light intensity in the spot by 3–4 orders of magnitude for 5–30

1. *Abbreviations used in this paper:* diI C14, 1,1'-ditetradecyl-3,3',3'-tetramethylindocarbocyanine; Fl-fab, fluorescein-conjugated Fab fragments; NBD-PC, 1-acyl-2-(12-[(7-nitro-2-1, 3-benzoxadiazol-4-yl)aminododecanoyl] phosphatidylcholine.

ms. The beam is again attenuated and used to determine the recovery of fluorescence in the bleached spot with time. Such experiments measure two parameters: D , a diffusion coefficient for mobile molecules, and M or R , the fraction of all labeled molecules mobile in the time of the experiment. Our computerized instrument for photobleaching has been described elsewhere (5).

The size of the laser spot used for measurements was varied by using objectives of different magnifications and numerical apertures. Further variation in spot size was achieved by defocusing the incoming laser beam so that it was slightly expanded when focused by a given objective. Laser spot radii were measured by scanning the image of a spot reflected from a carbon-coated glass surface, using a line analyzer (Colorado Video Inc., Boulder, CO). Scans were recorded on a strip chart recorder, and calibrated by comparison with scans of stage micrometers of known calibration. The laser beam is Gaussian, and a spot radius is defined as the distance from the center at which intensity is $1/e^2$ that of the maximum. Measured spot radii in our experiment ranged from 0.35 to 5 μm , with an error of $\sim 20\%$ in each measurement.

Cell Labeling for Photobleaching

24 h after plating onto coverslips, fibroblasts were washed in Hepes-buffered Hanks' balanced salt solution (HBSS) at 4°C . The washed cells were incubated at 4°C with 10 $\mu\text{g}/\text{ml}$ of NBD-PC or 20 $\mu\text{g}/\text{ml}$ F1-Fab in the same buffer for 30 min. Labeled cells were washed with cold HBSS and immediately used for fluorescence photobleaching recovery measurements. Labeled cells appeared ring-stained, with no visible internal fluorescence when examined in the fluorescence microscope. All fluorescence photobleaching recovery measurements were made at $18\text{--}20^\circ\text{C}$. Human skin fibroblasts are well-spread cells. All measurements could be made in membrane regions overlying cell cytoplasm, rather than those overlying the nucleus.

Photography of Labeled Cell Surfaces

Cells were labeled with NBD-PC as described above, or with diI C14, as described in reference 18. The limiting aperture and photomultiplier housing of the photobleaching microscope were replaced by a 35-mm camera and the laser spot produced by the $40\times$, NA 1.3 objective was increased to 6–12 μm by defocusing the laser before it reached the objective. The laser power was increased to about double that usually used. In one series of experiments a spot was photographed once, after being exposed to the laser spot for 30–50 s. In a second series, with laser power set at levels used for photobleaching, the spot was photographed, bleached, and rephotographed, and this series was repeated for a total of three or four bleaches. Images were captured on Tri-X film rated at ASA 1600. Despite this high rating, exposures required 20–40 s.

Results and Discussion

NBD-PC- and F1-Fab-labeled human skin fibroblasts appeared to be surface-stained when examined in the fluores-

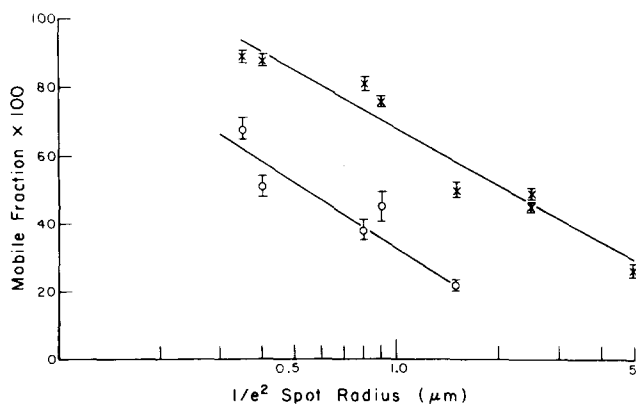


Figure 1. Mobile fraction of the lipid analog, NBD-PC (X), or of a protein label, F1-Fab (o), as a function of the $1/e^2$ radius of the laser spot used for measurement.

Table I. Mobile Fraction of Fluorescent Lipid and Protein Labels as Function of Laser Spot Radius

Objective	Beam radius μm	Label			
		NBD-PC		F1-Fab	
		Mobile fraction $\times 100^\ddagger$	n^*	Mobile fraction $\times 100$	n
10 \times (Defocused)	5.0	27 \pm 9	15	—	—
10 \times	2.5	49 \pm 8	21	—	—
22 \times (Defocused)	2.5	45 \pm 8	10	—	—
22 \times Water immersion	1.5	50 \pm 9	19	22 \pm 6	18
22 \times Oil immersion	0.9	76 \pm 5	30	45 \pm 15	15
40 \times Oil immersion	0.8	81 \pm 10	26	38 \pm 13	23
63 \times Oil immersion	0.4	88 \pm 13	83	51 \pm 17	45
90 \times Oil immersion	0.35	89 \pm 12	67	66 \pm 21	45

* Number of measurements.

‡ Standard deviation.

cence microscope, and showed no internal labeling. We measured the mobile fractions and diffusion coefficients of lipid and protein labels using eight different laser spots ranging in $1/e^2$ radius from 0.35 to 5 μm . We found that the mobile fraction of both NBD-PC and of F1-Fab was a function of laser spot size. The smallest spot bleached, 0.35 μm , gave the greatest mobile fraction, ~ 0.90 for NBD-PC and 0.70 for labeled membrane proteins. The largest laser spots used, 5.0 μm radius for lipids and 1.5 μm radius for proteins, gave the lowest mobile fractions, ~ 0.25 . The data for all measurements are summarized in Fig. 1 and details are given in Table I. It will be seen that the mobile fraction of label decreases monotonically for increasing laser spot size. The decrease of both NBD-PC and F1-Fab mobility correlates well with the increase in laser beam radius, $r > 0.95$.

The decrease in mobile fraction with increasing spot size could be due to any of the following: (a) bleaching of a significant and increasingly large fraction of the total labeled surface by the large laser beams; (b) selective heating of small spots compared to large spots; (c) optical artifacts, perhaps a function of the depth of focus of different objective, which vary with objective aperture; (d) labeling by the probes of discrete domains which cannot exchange label with their neighbors in the time of the experiment.

The first possibility is ruled out by the large size of the cells bleached. Our largest bleaching spot has an area of $\sim 80 \mu\text{m}^2$, while the smallest fibroblasts have a surface area of over $300 \mu\text{m}^2$ and the modal area of a population of fibroblasts is $\sim 1,500 \mu\text{m}^2$. Hence, depletion of a significant fraction of label when bleaching with the largest laser spot in our series could reduce the mobile fraction by a maximum of 25%. The next-largest spots have an area of only $\sim 20 \mu\text{m}^2$. Hence, the mobile fraction measured at these spot sizes, ~ 0.5 , cannot be explained by the bleaching of a significant fraction of surface label. We also note that the mobile fraction of other lipid labels is >0.9 regardless of the spot size used for measurement (Yechiel, E., and M. Edidin, manuscript in preparation).

Heating of the bilayer by the bleaching beam could in principle increase mobility of lipid probes. Using the method of Axelrod (2) we estimate the increase in temperature due to total absorption of the bleaching light in our smallest spot

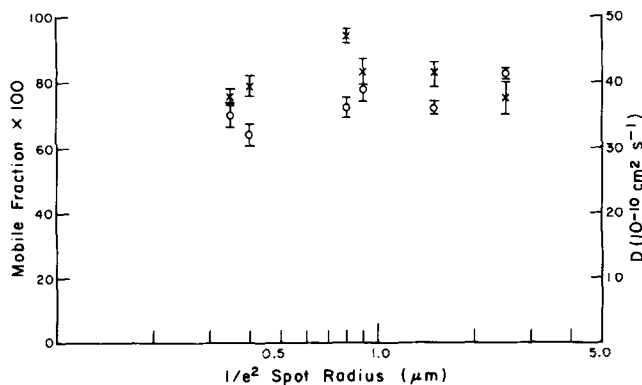


Figure 2. Mobile fraction (X) and diffusion coefficient (o) of NBD-PC incorporated into large liposomes (made from egg yolk lecithin).

is 0.2°C, given a laser power at the cell surface of 1 mW, and a 1% surface concentration of NBD-PC, with a molar extinction coefficient of 20,000. Thus the effects on probe mobility observed are not likely to be due to local heating.

We tested the possibility that the observed differences in mobile fraction are due to some unknown but systematic optical artifact due to the objectives, by measuring lateral diffusion of NBD-PC in large unilamellar liposomes. There was no significant difference between mobile fractions measured with spot radii ranging from 0.35 to 2.5 μm (Fig. 2). Hence, the mobile fractions measured in cell membranes (Fig. 1) are not likely to be artifacts of the measuring optics.

The observed decreases in mobile fraction of labels with increasing spot size do not appear to be artifacts of spot and cell geometry, or of the measuring optics. Our results then reflect the organization of membrane lipids and proteins. If our probes label lipids organized into discrete domains, and label proteins within these domains, then we would expect a decrease in mobile fraction as the radius of the measuring and bleaching spots exceeded the radius of the domains. The lower limit of mobile fraction expected will depend upon details of the membrane organization. If the membrane consists entirely of tightly packed domains, with 100% of the probe mobile within a domain, then to a first approximation the observed mobile fraction, M_{obs} , for large laser spot sizes

should depend upon domain and spot radii as $M_{obs} = \frac{r}{R}$, where r is the radius of the lipid domain and R is the radius of the measured spot. For measuring spots with radii much smaller than the domain radii, the observed mobile fraction should vary as $M_{obs} = \frac{r^2 - R^2}{r^2}$.

The fit of values predicted from these expressions to our experimental data suggests that domain radii are 1–1.5 μm. However, this estimate of domain size assumes domains of similar size, tightly packed, with no significant amount of lipid outside of domains. If this were so, then the diffusion coefficient measured with spots of different radii should be constant, as it is for NBD-PC in liposomes. The lateral diffusion coefficients estimated for NBD-PC in our experiments are in a range reported by others for diffusion of this probe in cell membranes (12). However, in our experiments, diffusion coefficients of NBD-PC increase with increasing laser spot radius, reaching a plateau for large spot sizes. This

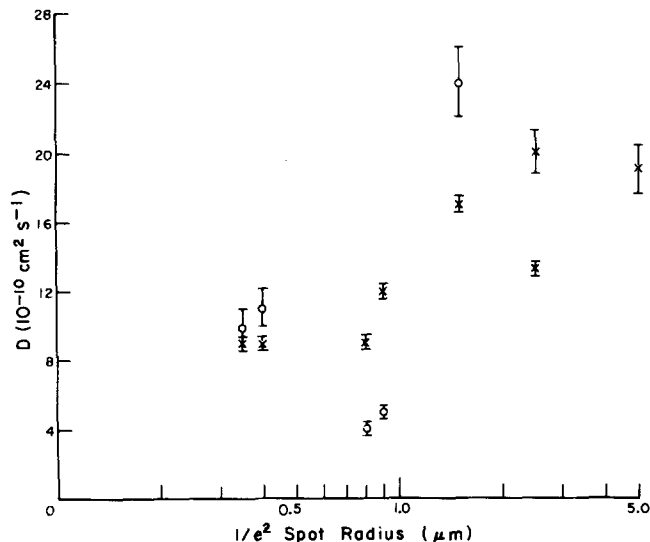


Figure 3. Lateral diffusion coefficients of NBD-PC (X) or FI-Fab (o) as a function of the $1/e^2$ radius of the laser spot used for measurement.

is shown in Fig. 3 and tabulated in Table II. (Diffusion coefficients for FI-Fab-labeled proteins also change with changing spot radius, but we have too few points to interpret the trends in this data set.) This result is expected if discrete domains are embedded in a lipid continuum in which all molecules are mobile. In such a case, the smaller diffusion coefficients measured with small laser spots would then represent an average for diffusion of NBD-PC in domains or in the lipid continuum in which they lie. A large laser spot would bleach entire domains lying completely within its area, and recovery of fluorescence in the bleached spot would be due to diffusion within partly bleached domains at the perimeter of the spot, and in the lipid continuum surrounding the domains (Fig. 4).

If the membranes we examined consist of discrete lipid domains surrounded by a larger continuum, and if the radii of the domains are larger than the radii of our smaller laser spots, then we expect that these small spots will either report lateral diffusion in the domains, or will report it in the region between them, or a mixture of the two, while larger spots

Table II. Lateral Diffusion Coefficients of Fluorescent Lipid and Protein Labels as a Function of Laser Spot Radius

Objective	Beam radius μm	Label			
		NDB-PC		FI-Fab	
		D*	n	D	n
10× (Defocused)	5.0	19 ± 6	15	—	—
10×	2.5	13 ± 2	21	—	—
22× (Defocused)	2.5	20 ± 4	10	—	—
22× Water immersion	1.5	17 ± 3	19	24 ± 9	18
22× Oil immersion	0.9	12 ± 3	30	5 ± 2	15
40× Oil immersion	0.8	9 ± 3	26	4 ± 3	23
63× Oil immersion	0.4	9 ± 5	83	11 ± 7	45
90× Oil immersion	0.35	9 ± 5	67	10 ± 7	45

* Diffusion coefficient units are $10^{-10} \text{ cm}^2 \text{ s}^{-1}$.

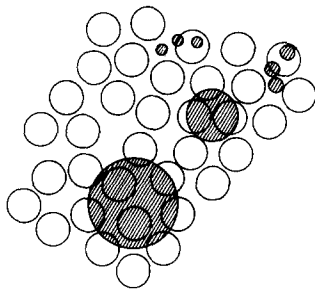


Figure 4. Domains in the fibroblast plasma membrane are represented by open circles. These appear to be $\sim 1 \mu\text{m}$ in diameter and are rich in proteins (see text). The region between domains forms a continuum over much, if not all, of the surface. The protein concentration is lower in this region than in the domains. Small and large laser spots (hatched circles) are superimposed on the model.

ought to consistently report diffusion averaged over both domains and interdomain regions with diffusion in the latter dominating measurements made with the largest spots (Fig. 4). Detailed analysis of the lateral diffusion coefficients measured with small laser spots further supports this idea. It will be seen from Table II that the variance of the means for diffusion coefficients, of both NBD-PC and Fl-Fab, measured with the smallest laser spots ($63\times$ or $90\times$ objectives) is much larger than the variance of all other measurements. This difference is evident when the distribution of diffusion coefficients measured at one of these spot sizes is compared with the distribution of diffusion coefficients measured with larger spots. Fig. 5 compares these distributions for NBD-PC diffusion. The distribution of diffusion coefficients measured with a $0.35\text{-}\mu\text{m}$ laser spot ($90\times$ objective (Fig. 5 a) is broad and differs significantly from a normal distribution when compared to such a distribution using the Kolmogorov-Smirnov test (7). The distribution of diffusion coefficients measured with a $2.5\text{-}\mu\text{m}$ radius laser spot ($10\times$ objective) (Fig. 5 b) is narrow and approximates a normal distribution. Other distributions, significantly different from the normal distribution, were found for diffusion coefficients of NBD-PC measured with a $0.4\text{-}\mu\text{m}$ spot radius ($63\times$ objective), and for diffusion coefficients of Fl-Fab measured with either small spot. These are reflected in the high SDs for these measurements (over 50% of the mean) in Tables II and III. The broad distributions are not likely to reflect cell-to-

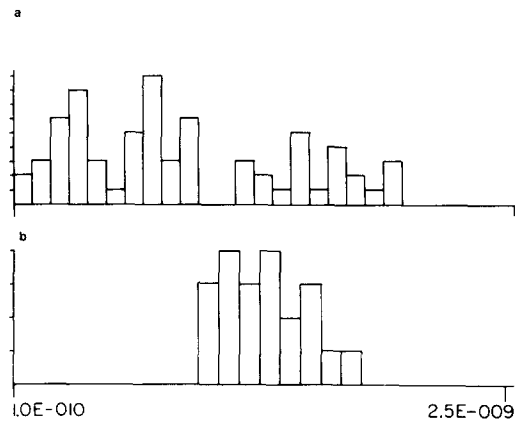


Figure 5. Distribution of lateral diffusion coefficients measured for NBD-PC using (a) a $10\times$ objective, producing a laser spot of $2.5\text{-}\mu\text{m}$ radius, or (b) a $90\times$ objective, producing a laser spot of $0.35\text{-}\mu\text{m}$ radius.

cell variations in D . Such variations ought to be detected with larger as well as with smaller laser spots. Rather, they reflect variations in the positioning of the spot on a given cell. We tested this by making 9–10 separate measurements of NBD-PC diffusion on each of six cells. Each group of 9–10 diffusion coefficients covered the same broad range as the 70–80 measurements made one per cell (Table II).

Diffusion coefficients, measured with small laser spots, are tabulated in Table III, and divided into three subgroups, together with values for mobile fractions and for intensity of labeling. The data indicate a direct relationship between intensity of NBD-PC labeling and diffusion coefficient, and an inverse relationship between intensity of Fl-Fab labeling and their diffusion. This relationship is clearly displayed in Fig. 6. The increased lateral diffusion of NBD-PC in regions of higher dye concentration might be due to the trivial fluidizing effect on membranes of high concentrations of the probe. However, the same distributions for diffusion of NBD-PC were found in separate experiments in which the level of labeling varied threefold (data not shown). Hence they are not liable to be artifacts of dye concentration in the

Table III. Comparison of Fluorescence Photobleaching Recovery Parameters Using $63\times$ and $90\times$ Objectives

Sample	Mean fluorescence intensity		D		Mobile fraction			
	NBD-PC	Fl-Fab	NBD-PC	Fl-Fab	NBD-PC	Fl-Fab		
	<i>n</i>	<i>n</i>						
Measured at small laser spot radii: $63\times$ objective – spot radius $0.4 \mu\text{m}$								
All measurements	83	45	57 ± 16	14 ± 5	9 ± 5	11 ± 7	88 ± 13	51 ± 18
Population I	24	18	79 ± 28	5 ± 1	15 ± 2	18 ± 3	88 ± 11	49 ± 17
Population II	35	12	59 ± 24	8 ± 5	9 ± 1	9 ± 2	89 ± 13	46 ± 15
Population III	24	15	34 ± 12	14 ± 6	4 ± 1	3 ± 1	86 ± 16	58 ± 18
Measured at small laser spot radii: $90\times$ objective – spot radius $0.35 \mu\text{m}$								
All measurements	67	45	48 ± 22	10 ± 5	9 ± 5	10 ± 7	89 ± 12	68 ± 21
Population I	22	13	68 ± 32	8 ± 2	16 ± 2	20 ± 4	87 ± 14	73 ± 18
Population II	24	20	52 ± 18	8 ± 2	8 ± 1	8 ± 2	91 ± 13	70 ± 22
Population III	21	12	24 ± 9	14 ± 5	4 ± 1	3 ± 1	89 ± 14	57 ± 18

* Thousands of counts per second \pm SD.

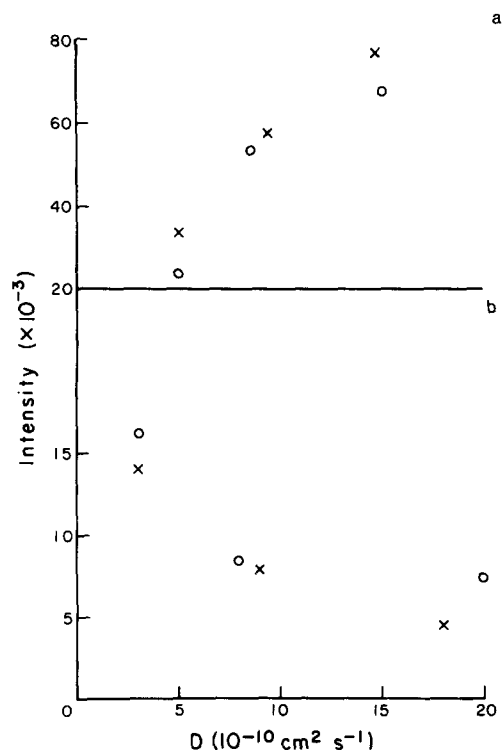


Figure 6. Lateral diffusion of NBD-PC (a) or Fl-Fab (b) as a function of concentration of label, expressed as intensity of labeling in the measured area. Measurements with the 63 \times objective (x); measurements with the 90 \times objective (o).

membrane. Instead, the relationships between degree of labeling and diffusion coefficient suggest that some regions of the membrane are enriched for proteins, while others are enriched for lipids. Since the diffusion coefficient of NBD-PC is largest when measured with larger laser spots, and these spots mainly report diffusion in the lipid continuum between domains, it seems that proteins are at higher concentration within the lipid domains than between the domains. Indeed, recent results on the interaction between membrane lipids and proteins in erythrocyte membranes (3, 14) suggest that interactions with membrane proteins might be important in organizing or stabilizing lipids in domains. One of us has previously discussed such a role for membrane proteins (20).

Our results give strong indications that fibroblast plasma membranes are organized into protein-rich lipid domains, separated by a protein-poor lipid continuum. The domains themselves are immobile on the time scale (tens of seconds) of our fluorescence photobleaching recovery experiments, but lipids and proteins within them are fully mobile. The apparent low mobile fractions observed for these molecules reflect the area of the laser spot used for bleaching and measuring recovery, relative to the area of the domains. The variations in diffusion coefficients measured with small laser spots, compared to that measured with larger spots, suggests that lipid domains in fibroblast membranes have radii larger than 0.4 μm though probably smaller than 1.5 μm .

Micrometer-scale domains should be visible if photographs or video images are made of labeled cells illuminated with a laser spot 5–10 μm in diameter, either comparing the

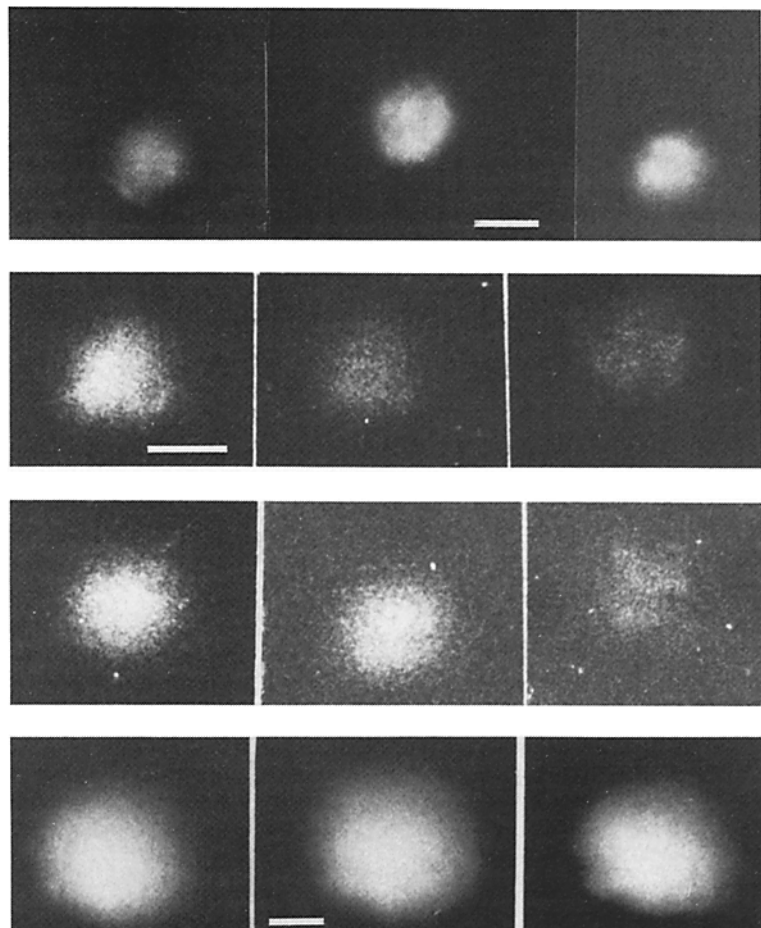


Figure 7. Images of NBD-PC- and diI C14-labeled cell surfaces illuminated by large laser spots. (Top row) NBD-PC spots that have faded for 40–50 s before photography; (Second and third rows) NBD-PC spots, before bleaching (left), after one bleach (center), and after four bleaches (right); (bottom row) diI C14 spots, before bleaching (left), after one bleach (center), and after three bleaches (right).

label before and after bleaching, or after a long period of fading. We have photographed a number of cells, labeled either with NBD-PC or with diI C14, one of the lipid analogs whose mobile fraction does not depend upon laser spot radius (Yeichiel, E., and M. Edidin, manuscript in preparation). We consistently find a coarse texture to spots on NBD-PC-labeled surfaces which is not seen in diI-labeled surface. A gallery of images illustrating these spots is shown in Fig. 7. The first series shows images of spots of NBD-PC that were slowly bleached by exposure to the attenuated laser beam at about twice the power used in photobleaching experiments. The apparent overall spot size is $\sim 12 \mu\text{m}$, and the spots are mottled by bright and dark patches that are several micrometers in extent. The second series shows two different spots of NBD-PC, $6 \mu\text{m}$ in apparent diameter, before bleaching, after a single bleach, and after a total of four bleaches. Before bleaching, the intensity of the spots is nearly uniform. After bleaching the spots appear to consist of light and dark regions. No such pattern was seen in images of NBD-PC solutions (not shown). The third series shows images of diI C14 made with the laser spot at the same size as was used in the second series. A uniformly intense central spot is seen, surrounded by a dimmer halo. DiI-labeled spots appear thus because the concentration of diI, and hence the distance from the center of the spot at which it is visibly excited by the Gaussian laser beam is greater than that of NBD-PC. The figure shows a spot before bleaching, after one and after three bleaches. Though there is some irregularity at the edge of the spot, it is largely featureless, even after repeated bleaches.

Thus we can produce images which are consistent with the predictions of our photobleaching results. Quantitative analysis of such spots will require both better digital video images, and a more rigorous mathematical model of a cell surface organized into micrometer-scale domains.

We thank Richard Cone (Department of Biophysics, The Johns Hopkins University, Baltimore, MD) for discussions and for reading the manuscript and Richard Pagano (Laboratory of Embryology, Carnegie Institution of Washington, Washington DC) for helpful suggestions.

This work was supported by National Institutes of Health grant AI14584 to Michael Edidin. This is contribution 1369 from the Department of Biology.

Received for publication 3 January 1987, and in revised form 23 March 1987.

References

- Ahlmers, W., and C. Stirling. 1984. Distribution of transport proteins over animal cell membranes. *J. Membr. Biol.* 77:169-186.
- Axelrod, D. 1977. Cell surface heating during fluorescence photobleaching recovery experiments. *Biophys. J.* 18:129-131.
- Devaux, P. F., and M. Seigneuret. 1985. Specificity of lipid-protein interactions as determined by spectroscopic techniques. *Biochim. Biophys. Acta.* 822:63-125.
- Edidin, M. 1984. Tissue architecture and lateral diffusion. *Comments Mol. Cell. Biophys.* 2:285-293.
- Edidin, M., and M. Zuniga. 1984. Lateral diffusion of wild-type and mutant L^d antigens in L cells. *J. Cell Biol.* 99:2333-2335.
- Frye, L. D., and M. Edidin. 1970. The rapid intermixing of cell surface antigens after formation of mouse-human heterokaryons. *J. Cell Sci.* 7: 319-335.
- Hogg, R. V., and E. A. Tannis. 1983. Probability and Statistical Inference. 2nd ed. Macmillan Publishing Co., New York. 407-412.
- Jacobson, K., E. Elson, D. Koppel, and W. Webb. 1983. International workshop on the application of fluorescence photobleaching techniques in cell biology. *Fed. Proc.* 42:72-79.
- Karnovsky, M. J., A. M. Kleinfeld, R. L. Hoover, and R. D. Klausner. 1982. The concept of lipid domains in membranes. *J. Cell Biol.* 94:1-6.
- Klausner, R. D., and D. E. Wolf. 1980. Selectivity of fluorescent lipid analogues for lipid domains. *Biochemistry.* 19:6199-6203.
- Kleinfeld, A. M., R. D. Klausner, R. L. Hoover, and M. J. Karnovsky. 1980. Lipid domains in membranes: evidence derived from structural perturbations induced by free fatty acids and lifetime heterogeneity analysis. *J. Biol. Chem.* 255:1286-1295.
- Morrot, G., S. Cribier, P. F. Devaux, D. Geldwerth, J. Davoust, J. F. Bureau, P. Fellman, P. Herve, and B. Frillet. 1986. Asymmetric lateral mobility of phospholipids in the human erythrocyte membrane. *Proc. Natl. Acad. Sci. USA.* 83:6863-6867.
- Oku, N., J. F. Scheerer, and R. C. MacDonald. 1982. Preparation of giant liposomes. *Biochim. Biophys. Acta.* 692:384-388.
- Porter, R. R. 1959. The hydrolysis of rabbit gamma globulin and antibodies with crystalline papain. *Biochem.* 73:119-126.
- Shen, B. W., R. Josephs, and T. L. Steck. 1986. Ultrastructure of the intact skeleton of the human erythrocyte membrane. *J. Cell Biol.* 102:997-1006.
- Singer, S. J., and G. Nicolson. 1972. The fluid mosaic model of the structure of cell membranes. *Science (Wash. DC).* 175:720-31.
- Wolf, D. E. 1986. Overcoming random diffusion in polarized cells—corralling the drunken beggar. *BioEssays.* 6:116-121.
- Wolf, D. E., W. Kinsey, W. Lennarz, and M. Edidin. 1981. Changes in the organization of the sea urchin egg plasma membrane upon fertilization: indications from lateral diffusion rates of lipid-soluble fluorescent dyes. *Dev. Biol.* 81:133-138.
- Wolf, D. E., M. Edidin, and A. M. Handyside. 1981. Changes in the organization of the mouse egg plasma membrane upon fertilization and first cleavage. Indications from the lateral diffusion rates of fluorescent lipid analogs. *Dev. Biol.* 85:195-198.
- Yeichiel, E., Y. Barenholz, and Y. I. Henis. 1986. Lateral mobility and organization of phospholipids and proteins in rat myocyte membranes. *J. Biol. Chem.* 260:9132-9136.